



HAL
open science

Sedimentation and preservation of the Miocene Atacama Gravels in the Pedernales-Chañaral Area, Northern Chile: Climatic or Tectonic Control?

Thierry Nalpas, Marie-Pierre Dabard, Gilles Ruffet, Antoine Vernon,
Constantino Mpodozis, Alfredo Loi, Gérard Hérail

► To cite this version:

Thierry Nalpas, Marie-Pierre Dabard, Gilles Ruffet, Antoine Vernon, Constantino Mpodozis, et al.. Sedimentation and preservation of the Miocene Atacama Gravels in the Pedernales-Chañaral Area, Northern Chile: Climatic or Tectonic Control?. *Tectonophysics*, 2008, 259, pp.161-173. 10.1016/j.tecto.2007.10.013 . insu-00334711

HAL Id: insu-00334711

<https://insu.hal.science/insu-00334711>

Submitted on 27 Oct 2008

HAL is a multi-disciplinary open access archive for the deposit and dissemination of scientific research documents, whether they are published or not. The documents may come from teaching and research institutions in France or abroad, or from public or private research centers.

L'archive ouverte pluridisciplinaire **HAL**, est destinée au dépôt et à la diffusion de documents scientifiques de niveau recherche, publiés ou non, émanant des établissements d'enseignement et de recherche français ou étrangers, des laboratoires publics ou privés.

Sedimentation/preservation of the Miocene Atacama Gravels in the Pedernales-Chañaral Area, Northern Chile: Climatic or Tectonic Control?

T. Nalpas¹, M.-P. Dabard¹, G. Ruffet¹, A. Vernon¹, C. Mpodozis², A. Loi³ and G. Hérail^{4, 5}

(1) Géosciences Rennes, Université de Rennes 1, UMR 6118 Campus de Beaulieu, 35042 Rennes cedex, France

(2) ENAP-SIPETROL, Av. Vitacura 2736, Las Condes, Santiago de Chile, Chile

(3) Dipartimento di Scienze della Terra, Università degli studi di Cagliari, Via Trentino 51, 09127 Cagliari, Italia

(4) IRD, LMTG. 14 Avenue Edouard Belin, Toulouse 31400, France.

(5) Dpto. Geología, Universidad de Chile, Plaza Ercilla 805, Santiago, Chile.

* Corresponding author. Tel.: 33 223235675; fax: 33 223236100. E-mail address:

thierry.nalpas@univ-rennes1.fr (T. Nalpas).

Abstract

In recent years, longitudinal changes on the thin/thick-skinned tectonic styles of the Central Andes has been intensively discussed while other studies have considered the role of mass transfers on the unloading the orogen, and on the stress regime along the plate interface arising from changes on the volume of sediment arriving into the Peru-Chile trench. The search for paleo-climate records is therefore crucial for our understanding of the history of the Central Andes. In this paper, we focus on the Atacama Gravels, an extensive blanket of Miocene continental deposits filling a Neogene paleo-valley system along the southern Atacama Desert in northern Chile. An east-west transect, between Pedernales and Chañaral (26°30'S), enabled us to carry out a sedimentological and tectonic study of the Atacama Gravels, based on logging and field observations along the Rio Salado canyon. New ³⁹Ar-⁴⁰Ar ages obtained on intercalated and overlying ignimbrites date the beginning of the Atacama Gravels sedimentation at around the Oligocene-Miocene boundary and cessation of sedimentation in the late Miocene. Thirteen lithofacies, included within five facies associations (A1 to A5) were identified. Depositional environments vary from proximal alluvial fan (A1, A2) in the Precordillera through ephemeral fluvial (A3, A4) to distal playa lake (A5) in the Coastal Cordillera. No evidences

of syn-sedimentary deformation have been found, showing that the change from sediment removal to sediment preservation cannot be explained by tectonic causes, and climate change appears to be the dominant controlling factor of sediment preservation. A progressive change from semi-arid towards hyper-arid climatic conditions during the Miocene, led to a reduction on the transport capacity of the fluvial system and sediment preservation along the paleovalley system formed during the Oligocene.

Keywords: Atacama Gravels; Andes; depositional environments; climate; deformation; ^{39}Ar - ^{40}Ar datation.

1. Introduction

The links between deformation and climate in orogenic systems have been intensely debated for more than a decade (e.g. Molnar and England, 1990; Lamb and Davis, 2003). Recent studies show that changes in the magnitude of mass transfer from the Andean range to the trench across different climate zones must be considered to explain north-south variations in tectonic style (Alpers and Brimhall, 1989; Hartley et al., 2000; Montgomery et al., 2001). Variations in the intensity of mass transfer processes may influence the location of compressive deformation, thus influencing the relief and climate (Beaumont et al., 1992; Summerfield and Hulton, 1994; Avouac and Burov, 1996; Mugnier et al., 1997; Leturmy et al., 2000; Nalpas et al., 2003). Lamb and Davis (2003) have suggested that the aridity observed at the latitude of the Atacama Desert is the cause rather than the consequence of the Andean plateau uplift, because sediment shortage in the Chile trench may affect the force balance in the South American plate by increasing the shear stress against the subduction surface.

In this paper, we focus on an extensive blanket of Miocene continental sediments described in the literature as the Atacama Gravels (AG, Mortimer, 1973; Cornejo et al., 1993; Hartley et al., 2000). Our aim is to determine the factors responsible of their preservation, which can be: i) tectonic, with creation of a physical barrier or ii) climatic, with a decreasing of mass-transfer towards the ocean. A detailed sedimentological study was performed in the Chañaral-Potreros region (26°30'S, Figs. 1 and 2), along the Rio Salado catchment area, from the Precordillera, to the Coastal Cordillera and a sedimentological model is proposed. ^{39}Ar - ^{40}Ar dating was performed on interbedded ignimbrites.

Correlations between the sections, based on radiometric ages and facies evolutions, are proposed and the evolution of mass transfers during the Miocene is considered.

2. Geological setting

The evolution of the Andean orogen, since the Jurassic, has been governed by the subduction of the oceanic Farallon (Nazca) plate beneath the South American continent (Coira et al., 1982; Mpodozis and Ramos, 1989). The main phases of deformation have been generally related to changes in the convergence rate and/or absolute westward motion of the South American plate (Pardo-Casas and Molnar, 1987). Since the Late Miocene, most of the shortening in the Central Andes has been concentrated in the thin-skinned Sub Andean fold and thrust belt (Gubbels et al., 1993; Echavarría et al., 2003; Allmendinger et al., 1997; Baby et al., 1997; Kley et al., 1999; McQuarrie et al., 2005), contemporaneously with the rise of the Altiplano-Puna high plateau to elevations of more than 4000 m (Gregory-Wodzicki, 2000; Garzión et al., 2006; Ghosh et al., 2006). In contrast, the northern Chilean fore-arc in the southern Atacama Desert region seems to have been a much more stable tectonic domain recording only minor Neogene horizontal shortening (Cornejo et al., 1993; Godoy and Lara, 1998; Mpodozis and Clavero, 2002; Audin et al., 2003; Riquelme et al., 2003; Arriagada et al., 2006).

Along the Chañaral-Pedernales transect, the western slope of the Andes comprise six morphotectonic units (Fig. 1): the Coastal Cordillera along the Pacific coast, the Central Depression, the Precordillera, the Pre-Andean Depression (including the Pedernales-Maricunga basins), and finally the Cordillera Claudio Gay, bordering the modern volcanic arc of the Western Cordillera and the Puna plateau located further to the east. The geology along the studied transect is dominated by a series of east-stepping Mesozoic and Cenozoic magmatic arcs (Mpodozis and Ramos, 1989; Arriagada et al., 2006). The Coastal Cordillera consists of the eroded remnants of the early lower Jurassic to lower Cretaceous Andean arc, with large plutonic complexes, a Jurassic andesitic to basaltic volcanic sequence (La Negra Formation) and upper Jurassic to lower Cretaceous andesitic to dacitic lavas (Punta del Cobre Group, Dallmeyer et al., 1996; Lara and Godoy, 1998). The main tectonic feature in this Cordillera is the Atacama Fault System (Salado Segment, Brown et al., 1993; Grocott and Taylor, 2002), which was formed in the Jurassic as a trench-linked structural system along the axis of the early Andean magmatic arc. The rare outcrops of bedrock in the Central Depression are dominated by upper Cretaceous

andesitic volcanic and sedimentary sequences (Llanta Formation) unconformably covered by Paleocene to lower Eocene volcanic complexes (Cornejo et al., 1993 and 1997; Iriarte et al., 1996). Further east, Jurassic to lower Cretaceous back-arc marine and continental sedimentary units overlie upper Paleozoic igneous basement units (Cornejo et al., 1993). In the western part of the Precordillera, around El Salvador and Potrerillos (Fig. 2), the Mesozoic back-arc sediments are intruded by Eocene sub-volcanic stocks and porphyries spatially related to the Eocene to Early Oligocene Sierra del Castillo-Agua Amarga faults, and the Potrerillos Fold and Thrust Belt (Mpodozis et al., 1994; Tomlinson et al., 1994 and 1999). The Pre-Andean Pedernales and Maricunga basins, located along the eastern edge of the Precordillera (Fig. 1) record a younger volcanic activity dated as Oligocene-Miocene (Cornejo et al., 1993; Mpodozis et al., 1995). To the east, the Cordillera Claudio Gay is formed by an uplifted Paleozoic basement block, covered by Eocene to Miocene sedimentary and volcanic sequences (Mpodozis and Clavero, 2002) which makes up the western boundary of the Western Cordillera formed by the partly active chain of stratovolcanoes and caldera complexes of the Central Andean Volcanic Zone (CVZ), rising well above 6000 m (Kay et al., 1999; Clavero et al., 2000). Eocene deformation with tectonic uplift and the consequent denudation focused in the Precordillera, produced a large amount of sediments now preserved to the east of the CVZ in the Argentine Puna (Kraemer et al., 1999; Coutand et al., 2001; Voss, 2003), and to the west, along Cordillera Claudio Gay and Pre-Andean Depression (Cornejo et al., 1998b; Mpodozis and Clavero 2002). Further west, semi-consolidated sequences of Neogene gravels (Atacama Gravels, AG, Sillitoe et al. 1968; Mortimer, 1973; Cornejo et al., 1993 and 1998a; Riquelme, 2003) are distributed over an area from the Precordillera to the Coastal Cordillera (Fig. 2). The onset of sedimentation was assigned to the base of the middle Miocene, as indicated by the K/Ar (biotite) ages obtained on ignimbrites intercalated in the AG sequence at Quebrada Doña Inés Chica and Cuesta del Jardín (15.3 ± 1.5 Ma / Cornejo et al., 1993). In the Precordillera, the top of the Atacama Gravels is sealed by an extensive pediment surface (Atacama pediplain) covered by the regionally widespread San Andrés Ignimbrite (SAI, attributed to the upper Miocene, dated by K/Ar on biotite (9.6 ± 0.4 Ma / Clark et al., 1967; Sillitoe et al., 1968; Mortimer, 1973; Cornejo et al., 1993). These ages are similar (within errors) to the 9 Ma exposure age measured by Nishiizumi et al. (2005) from cosmogenic nuclides (^{10}Be , ^{26}Al , and ^{21}Ne) on cobbles sampled on the pediment surface.

3. Atacama Gravels: facies associations and depositional environments

As part of the present study we carried out a detailed sedimentological study of the AG along the El Salado valley including the analysis of 15 sedimentological logs (Fig. 2) and the mineralogical composition of selected samples (Table 1). Thirteen lithofacies (according to the facies codes of Horton and Schmitt, 1996 and Miall, 1996; except for the L facies) were identified (Table 2). Facies were grouped into five facies associations.

3.1. Composition of the Atacama Gravels

In the coarse facies, most of the elements are made up of andesitic fragments, nevertheless, plutonic elements and sedimentary elements, specially limestone fragments, are present in the Precordillera (log 1) and in the Central Depression (log 2 and log 3). In the sandy facies (Table 1), lithic fragments are mainly represented by volcanic clasts while sedimentary and plutonic rock fragments are less abundant. The volcanic clasts show various textures (felsitic, microlitic, intergranular and intersertal textures) implying inputs from volcanic formations of silicic to basaltic composition. Some of these fragments show evidence of hydrothermal alteration. A contribution of plutonic and/or metamorphic sources is documented by the presence of fragments made up of quartz and feldspars (potassic feldspath and/or plagioclase), quartz and micas as well as orthoclase and microcline monominerals. Limestone clasts including bioclastic, oolitic and crystalline types are also present.

The potential source areas of clastic material (volcanic, plutonic) are widely distributed across the studied transect from the Precordillera to the Coastal Cordillera. The calcareous formations (Jurassic and Cretaceous), actually outcrop in the thrust belt bounding the Precordillera and the Salar de Pedernales. The occurrence of sedimentary clasts in the Central Depression implies that part of the input is derived from the Precordillera.

3.2. Facies associations

3.2.1. A1 facies association: Gmm, Gcm, Sh, Sm and Fm (Figs. 3 and 4)

Description: This association is mainly composed of Gmm and Gcm facies, with intercalations of Sm, Sh and Fm. These poorly sorted gravels form thick (from one dm to several metres thick), extending laterally up to several tens of metres and devoid of internal stratification. The basal surfaces of these units are sharp and sometimes erosive. In the Gmm facies, the matrix is sandy. The clasts are angular (Gmm) to sub-rounded

(Gcm), with a diameter between 1 and 40-50 cm. The beds of fine to coarse sand (Sh and Sm) extend laterally to a few metres and are 5 to 20 cm thick with scattered gravel lenses. These facies are sometimes associated with thin (several cm) layers of mud and silt with mudcracks (Fm facies).

Interpretation: The Gmm and Gcm facies represent cohesive flow deposits, sub-aerial to sub-aqueous debris-flows, or (Gcm) deposits from hyper-concentrated density flows (Smith, 1986; Horton and Schmitt, 1996; Miall, 1996; Mulder and Alexander, 2001). The Sh facies, characterized by horizontal lamination, is deposited under upper-flow regime conditions (Collinson, 1986; Miall, 1996). It is interpreted as representing sheetflood deposits (Horton and Schmitt, 1996), and the geometry of the beds indicates an accumulation from unconfined or poorly confined sheetfloods. The Sm facies is interpreted as being deposited from hyper-concentrated flows (Smith, 1986) or high-density turbidity currents (Horton and Schmitt, 1996) where the sand deposition is too rapid to allow the development of bedforms. The Fm facies is interpreted as sub-aerial waning flood flows (Miall, 1977).

3.2.2. A2 facies association: Gcm, Gcn, Gh, Sh, Sm and Fm (Figs. 3 and 4)

Description: This association is made up of gravels (Gcn, Gh and Gcm facies) with clasts up to 20 cm in diameter. Sandy beds (Sm, Sh and Fm facies) and wind faceted pebbles are more abundant than in the A1 association. The stratification is noticeable as a layering of very elongated lens-shaped sediment bodies. The lateral extension of the beds varies from one to several tens of metres, with cm to dm-scale thickness. The beds of Gcn facies show an erosive basal surface with basal imbricated clasts capped by pebbles and granules with fining-upward grading. The Gh facies is made up of the stacking of well-sorted thin beds (several cm thick) of sub-rounded to sub-angular gravels containing imbricated clasts and horizontally aligned flattened clasts. Intercalations (20 – 30 cm thick) of fine- to coarse-grained sand and silt facies (Sh, Sm and Fm) are common. A few beds are characterized by a brick-red surface coloration. Horizontal and vertical gypsum-filled cracks are present, while roots casts and remnants of organic matter can be observed locally.

Interpretation: The depositional processes involved in the formation of the Gcm, Sm, Sh and Fm facies are described in the A1 Association. In the Gcn and Gh facies, the imbrication of clasts suggests that part of the sedimentation process involves bedload traction. These facies are formed in stream-flows, hyper-concentrated flows (Waresback and Turbeville, 1990; Svendsen et al., 2003) or high-density turbidity currents (Horton and

Schmitt, 1996). The Gcn facies is found in channel fills, channel-lag sheets and channel-bar sheets (Nemec and Postma, 1993). The Gh facies is deposited under upper-flow regime conditions (Waresback and Turbeville, 1990) and is interpreted as being deposited from unconfined or poorly confined sheetfloods (Horton and Schmitt, 1996). The gypsum-filled cracks can be compared to those described by Kocurek and Hunter (1986) and Hartley and May (1998) as the result of post-deposition desiccation.

3.2.3. A3 facies association: Gh, Gpt, Sh, Spt and Fm (Figs. 3 and 4)

Description: This facies association consists of well-sorted medium to coarse sand and sub-rounded to rounded gravels (granules to pebbles). It includes horizontally stratified deposits (Gh and Sh), grading vertically or horizontally into planar and trough cross-bedded facies (Spt and Gpt). The Gh and Sh facies are associated together in units several dm to several metres thick, extending laterally up to several tens of metres. The Gh facies contains numerous levels with horizontal clast alignments. The Spt and Gpt facies form lens-shaped bodies, about 5 to 30 cm thick and several metres wide. The basal surfaces can be erosive, overlain by flattened granules and imbricated clasts. Rare intercalations of Gcm facies form beds about 10-20 cm thick. Rare, thin and discontinuous intercalations of Fm facies are also observed.

Interpretation: The sheetflood facies (Gh and Sh) are similar to those already described, being derived from unconfined flows. A notable feature of this association is the episodic presence of Gpt and Spt facies, which may correspond to channel infill deposits associated with transverse and lingoid bars or with 2D-3D dunes (Miall, 1996; Bordy and Catuneanu, 2001; Uba et al., 2005). The presence of thin intercalations of the Fm facies implies confined flows in a shallow-water environment.

3.2.4. A4 facies association: Gcm, Gcn, Sh, Sm and P (Figs. 3 and 4)

Description: This association is mainly made up of Sh and Sm facies with some intercalations of Gcm and Gcn facies. Sh and Sm facies form units several metres thick, without visible lamination. Occasional horizons, 1 to 5 cm thick and extending across several metres, are cemented by carbonate (P facies). The Gcm and Gcn facies form lenticular beds with a lateral extension of one to several metres and a thickness varying from 0.1 to 1 m. Their basal surface is gently erosive. A few imbricated clasts and a few horizontally aligned clasts occur in the Gcn facies.

Interpretation: Sh, Sm and Gcn facies imply unconfined and confined (Gcn) stream-flows. The intercalations of Gcm facies are linked to debris-flows. The carbonate horizons may

be related to cementation of sandy facies from evaporation capillary groundwater flow (Miall, 1996).

3.2.5. A5 facies association: Sn, Fmh, L and P (Figs. 3 and 4)

Description: One end-member of this association is dominated by the Fmh facies, composed of brown-red clays associated with halite and some gypsum. Some tepee structures are present. Intercalations of thin (several cm) bio-micritic beds (facies L) are present containing dislocated ostracod valves. The second end-member of this association is made up of fining-upward sand sequences (facies Sn), which are 30 to 60 cm thick. The basal surfaces of these units are slightly erosive, and the grain size ranges from gravel to coarse sand, fine sand and silt. This facies contains some indurated carbonate horizons (facies P). Bioturbation (i.e., root traces and some burrows) is present in the upper parts of the sequences.

Interpretation: The Fmh facies results from the deposition of clays from suspension, associated with the precipitation of evaporites in a stagnant saline water body. Detritic limestone intercalations are linked to periods with no terrigenous input, allowing colonization by ostracods. The Sn facies is interpreted as fining-upward sequences deposited from hyper-concentrated flows (Smith, 1986; Horton and Schmitt, 1996) or from high- or low-density turbidity currents (Ghibaudo, 1992). Each sequence can be related to a single depositional event, as indicated by the grading. The absence of clay beds at the top of the sequences suggests immediate water seepage. The presence of root traces implies an occasional colonization by vegetation between floods.

3.3. Depositional environments

The facies associations recognized in the Atacama Gravels can be placed along a continuous depositional profile (Figs. 4a and 4b), passing westwards from alluvial fan (A1 and A2 associations), through ephemeral fluvial (A3 and A4 associations), to playa environments (A5 association).

3.3.1. Alluvial fan environment

This environment is represented by the A1 and A2 associations. The A1 association is mainly made up of thick units resulting from the stacking of successive deposits from high-density flows (Gmm and Gcm facies). In the A2 association, the stream flow processes are dominant and are expressed by Sh, Gh, Gcn and Sm facies intercalations

whose sheet-like geometry indicates deposition from unconfined or poorly confined sheetfloods. The absence of ripple cross-lamination on the upper surfaces of the sandy beds indicates rapidly waning flows with no stage-reactivation of the sediment. These facies are interpreted as the result of high-energy flood deposition in a shallow water body. The only evidence of steady water body is provided by the rare Fm facies intercalations, with mudcracks indicating mud decantation and desiccation. The scarcity of this facies and of channelled stream deposits (Gcn facies) suggests that flashfloods are the dominant processes in this environment rather than steady water currents. Periods of relative stability accompanied by soil development are expressed by the rubefaction of some sandy and silty layers as well as the root casts observed in the A2 association.

The shift from the A1 debris-flow-dominated association to the A2 sheetflood-dominated association is accompanied by an overall decrease in grain size and an increase in the lateral extension of beds. Several factors can be invoked to explain such an evolution: an increase of the distance to the source area, a change in bedrock lithology, a variation in the vegetation cover, climat evolution or a decrease of the fan slope (Blair and McPherson, 1994; Levson and Rutter, 2000; Spalletti and Piñol, 2005). In a sedimentological model of alluvial fan, these two facies can represent the proximal (A1 association) – distal (A2 association) trend.

3.3.2. Ephemeral fluvial environment

This depositional environment is composed of the A3 and A4 facies associations. They comprise sheetflood sand and fine gravel facies (Sh, Sm and Gh), with intercalations of channel infill (Spt, Gpt and Gcn) and minor occurrences of debris-flows (Gcm facies). These features suggest a stream-flow dominated environment, subject to unconfined, high-particle-density flows together with more diluted flows (Spt and Gpt facies). The A3 association, which contains the channel infill facies, can be linked to a shallow braided system possibly resulting from low-magnitude events reworking the surface of larger flood units. However, the scarcity of channel infills and of fine-grained sediment intercalations is compatible with sudden and ephemeral flows followed by rapid seepage. In the depositional profile, this environment is located downstream of the alluvial fan.

3.3.3. Playa lake environment

This environment corresponds to the A5 association. The Sn facies, linked to unconfined ephemeral flows discharging into a standing water body, could represent fringe deposits. The lack of clay deposits at the top of the Sn sequences implies rapid seepage

and aerial exposure. The Fmh and L facies represent deposits from a water body. The Fmh facies results from the settling out of fine particles associated with the precipitation of evaporite minerals. It is characteristic of mudflats (Hartley and May, 1998) and is more distal than the Sn facies. The carbonate intercalations (L facies) with well-preserved bioclasts represent low-energy episodes without terrigenous inputs.

4. Arrangement of facies associations and stratigraphic correlations

4.1. ³⁹Ar-⁴⁰Ar dating of ignimbrites

The two ignimbrite layers interbedded in log 1 have already been dated by K/Ar on biotite (Clark et al., 1967; Mortimer, 1973; Cornejo et al., 1993). Nevertheless, to establish correlations between the different logs, new radiometric dating by ³⁹Ar-⁴⁰Ar method, have been performed on all the ignimbrites layers intercalated in the logs. In the same time ignimbrites located along the Rio Salado Valley (Pampa del Inca), more in the North (Quebrada Doña Inés Chica) and more in the South (Quebrada Chañaral Alto) were dated (Fig. 2).

4.1.1. Analytical procedure

Eight ignimbrite samples (02 to 08GA05 and IGA 1-04) were analysed with an ³⁹Ar-⁴⁰Ar laser probe (CO₂ Synrad®). Analyses were performed on single grains of sanidine and/or biotite with a duplicate for sample 03GA05. Sanidine and biotite minerals were carefully handpicked under a binocular microscope from crushed ignimbrites (0.3-2 mm fraction). The samples were wrapped in Al foil to form packets (11 mm × 11 mm × 0.5 mm), which were stacked up to form a pile. Flux-monitoring packets were inserted every 10 samples. The stack was placed in an irradiation can, irradiated for 13.33 hours (integrated power 40 MWH) at the McMaster reactor (Hamilton, Canada) with a total flux of 1.2×10^{18} n.cm⁻². The irradiation standard was sanidine TCR-2 (28.34 Ma according to Renne et al., 1998). The sample arrangement allowed us to monitor the flux gradient with a precision of ±0.2%.

The step-heating experimental procedure has been described in detail by Ruffet et al. (1995, 1997). Blanks were performed routinely each first or third run, and then subtracted from the subsequent sample gas fractions. Analyses were performed on a Map215® mass spectrometer.

To define a plateau age, we required a minimum of three consecutive steps, corresponding to a minimum of 70% of the total $^{39}\text{Ar}_K$ released. Under these conditions, the individual fraction ages should agree to within 1σ or 2σ of the integrated age of the plateau segment. All ^{39}Ar - ^{40}Ar results discussed here are expressed at the 1σ level.

4.1.2. Results (Table 3 and Fig. 5)

All analyses were suitable for calculating plateau ages (Fig. 5b to f). Three events were evidenced.

First event

Duplicate runs performed on two single grains of biotite from sample 03GA05 (Fig. 5b) yield highly reproducible age spectra with a slight increase of apparent ages in the last 60% of $^{39}\text{Ar}_K$ degassing. Isochron age calculations (correlation diagram technique ($^{36}\text{Ar}/^{40}\text{Ar}$ versus $^{39}\text{Ar}/^{40}\text{Ar}$) (Turner, 1971; Roddick et al., 1980; Hanes et al., 1985), yield very discordant results, with ages ranging up to ca. 29 Ma. The corresponding $(^{40}\text{Ar}/^{36}\text{Ar})_i$ ratios, which can be as low as ca. 246, indicate that the calculated regressions are really errorchrons, so the calculated isochron ages are not valid. Analysis of a plagioclase single grain (Fig. 5b) from the same sample yields a plateau age of 15.5 ± 0.8 Ma, corroborated by a concordant isochron age at 15.7 ± 1.1 Ma (Table 3). Age concordance between biotites and plagioclase from sample 03GA05 suggests the existence of an eruptive event at ca 16.3 Ma (Fig. 5a).

Second event

Most of analysed samples (6 among 8) display plateau ages in the range 9.46 ± 0.05 Ma to 9.15 ± 0.02 Ma, on single grains of biotite or sanidine (Fig. 5c to e). Two samples, 02GA05 and 04GA05, show slightly discordant biotite and sanidine plateau ages (Fig. 5c and d). These two samples yield the oldest plateau ages, at ca 9.45 Ma. Using the isochron age calculation method, we obtain slightly younger discordant ages in the range 9.34 ± 0.08 Ma to 9.12 ± 0.02 Ma (Table 3). Again, the oldest ages (9.34 ± 0.08 Ma and 9.25 ± 0.06 Ma) are obtained from samples 02GA05 and 04GA05, with $(^{40}\text{Ar}/^{36}\text{Ar})_i$ ratios of 286.3 ± 10.1 % and 303.6 ± 0.6 %, respectively. These initial ratios and corresponding slightly older plateau ages suggest that these two samples could contain a small excess argon component. Thus, we can assume that these 6 samples date a single eruptive event at ca. 9.1-9.2 Ma (Fig. 5a).

Third event

The youngest age is displayed by a sanidine grain from sample 06GA05 (Fig. 5f). The plateau age at 5.97 ± 0.07 Ma is concordant with the isochron age at 5.86 ± 0.12 Ma. These results suggest the existence of an eruptive event at 5.9-6.0 Ma (Fig. 5a).

These new analyses provide ages that appear distinct in comparison with previously published data. Hence, the lowermost ignimbrite of Log 1 (Figs. 2 and 6), named "Los Cristales" (LCI) in the "Cuesta el Jardin" (Cornejo et al., 1999), yields an age of ca 16.3 Ma, whereas it was previously dated at 15.3 ± 1.5 Ma (Cornejo et al., 1993). The San Andrés ignimbrite is dated here at 9.1-9.2 Ma, in a good agreement with the age of 9.19 ± 0.61 Ma obtained by Riquelme et al. (2007), and slightly younger than the age of 9.6 ± 0.4 Ma previously obtained (Clark et al., 1967; Mortimer, 1973; Cornejo et al., 1993).

4.2. Log correlations

4.2.1. Log descriptions

In the Precordillera, log 1 displays 400 m of sediments preserved in a paleovalley, lying above a volcanic basement. The morphology of the basement/sediment contact changes from a surface smoothed by water flow near the paleovalley floor, to a progressively much rougher surface going upwards along the paleovalley slopes which possibly reflecting a decreasing water-flow as sedimentation progressed (Fig. 6). This paleovalley is filled by 350 m of coarse sediments accumulated in an alluvial fan environment (A1 and A2 associations). The Los Cristales ignimbrite, dated at ca 16.3 Ma, overlies these deposits and is itself covered by 50 m of sediments accumulated in an ephemeral fluvial environment (A3 association). The San Andrés Ignimbrite, dated at 9.1-9.2 M, occurs above this facies association sealing a sub horizontal erosional surface and forms the topmost unit of the log 1. Paleocurrent measurements carried out in the different facies associations show a constant flow direction towards the SW (Fig. 2).

Three logs (2, 3, and 6) were drawn up in the Central Depression. Although the bases of logs 3 and 6 are not visible, gravimetric studies (Gabalda et al., 2005) have provided detailed informations on the geometry of the basement/sediment interface between these two logs. These data suggest that this zone corresponds to a weakly incised paleovalley filled by 150-200 m of gravels (Gabalda et al., 2005). The base of log 3 is represented by around 70 m of coarse deposits, accumulated in alluvial fan environment (A1 and A2 associations), with paleocurrent directions towards the SW (Fig. 2). As found at log1, these deposits are capped by a pediment surface, which

can locally correspond to a period of non-deposition or erosion, and is sealed by the San Andrés Ignimbrite (9.1-9.2 Ma). The topmost 30 m of this log section consist of sediments deposited in a fluvial environment (association A3).

Log 2, which is not represented in Fig. 6, is located to the east of log 3 (Fig. 2), is made up by 30 m of sediments lying directly on the volcanic basement. These deposits were laid down in a fluvial environment (association A3). Near the base, paleocurrents are directed towards the SW (Fig. 2), but change to the NW at the top. Log 6 comprises 30 m of sediments accumulated in a fluvial environment, showing a progressive lateral transition between facies associations A4 and A3. Paleocurrents are directed towards the NW and the upper part of the section is formed by outcrops of the San Andrés Ignimbrite (9.1-9.2 Ma).

Logs 9, 12 and 15 were drawn up in the Coastal Cordillera. Although the contact with the substratum is only visible in log 9, the proximity of the basement and its slope in logs 12 and 15 allows to estimate the depth of the basement/sediment contact to within a few metres. The base of these three logs is made up of relatively fine-grained facies (sand to clays) deposited in a playa lake environment (A5 association). Massive or poorly bedded coarse deposits with angular pebbles rest on an erosional surface that overlies the fine-grained facies. These coarse deposits are formed by the Gmm facies and especially Gcm facies. They contain andesitic clasts and reworked the underlying sediments. Paleocurrent measurements carried out in these fans yield NE flow directions for log 12 and NW for log 15 (Fig. 2). These deposits can be interpreted as laid down in local alluvial fans. They are overlain by an ignimbrite dated at 5.9-6.0 Ma.

4.2.2. Correlations between logs

Six of the more representative 15 AG logs studied along the Chañaral-Potrerrillos transect are shown in Figure 6. The log 1 and the log 3, located respectively in the Precordillera and in the Central Depression, belong to distinct systems. They are separated by an area of high relief, the Sierra del Caballo Muerto (Fig. 7) and the log 1 is located in a NE-SW-trending paleovalley, which corresponds to the present-day valley of the Quebrada del Caballo Muerto. This paleovalley joins up with the one intersected by log 3 to form a single paleovalley in the Central Depression (Rio Salado, Fig. 2). The correlation between these two logs can only be based on the radiometric data.

The logs 2 to 15, which correspond to the filling of the same paleovalley (Rio Salado) can be correlated on the base of sedimentary facies and the available radiometric data. In

figure 6, the logs are aligned with the upper surface of the Atacama Gravels (Atacama paleo-surface) which decreases continuously in elevation westwards, from about 2700 to 400 m.

In the Precordillera, the facies associations of log 1 show an evolution from alluvial fan facies (A1-A2) deposited before the emplacement of the Los Cristales Ignimbrite (16.3 Ma, Fig. 6) to fluvial facies (A3) deposited between 16 and 9 Ma (the age of the San Andrés Ignimbrite, Fig. 6). This tendency correspond to a global retrogradation of the system. A same retrogradation trend is observed in the log 3 (Central Depression) with alluvial fan facies (A1-A2) overlaid by fluvial facies. The particular position of log 3, on the western flank of the Sierra Caballo Muerto (Fig. 7), explains the presence of proximal facies pre-dating 9.1-9.2 Ma. The radiometric data reveal the lateral passage from alluvial fan association in the log 3 towards fluvial facies in the log 6 (Fig. 6). Paleocurrent measurements at logs 2, 3 and 6 yield SW-NW-trending directions, consistent with an overall spreading of sediment from the Precordillera towards the coastal region. Between log 6 and log 9, the geometry of the Atacama Gravels, with a generally westward dipping, suggests a lateral passage from fluvial facies in the Central Depression to playa-lake facies in the Coastal Cordillera.

In the Coastal Cordillera, the local fans result from the erosion of hills bordering the Río Salado paleovalley (volcanic and plutonic clasts) and underlying gravels (AG clasts). They form a series of independent sedimentary bodies as shown by changing paleocurrents directions (Fig. 2). The presence of an ignimbrite dated at 5.9-6.0 Ma, located at the top of the local fan in log 12, leads us to suggest a late-stage (post 6 Ma) local incision of the El Salado system at the level of the Coastal Cordillera. On the other hand, dating of the pedimentation surface in the Precordillera (Nishiizumi et al., 2005) and the presence of the San Andrés Ignimbrite in eroded valleys in this area (Riquelme et al., 2007), seem to indicate an early stage of incision in the Precordillera.

5. Discussion

5.1. Preservation of the Atacama Gravels: Tectonic or climatic control?

Some sedimentary features of the Atacama Gravels provide information on the prevailing climatic conditions during sedimentation. Upper-regime stream-flow deposits are very common in the proximal and median facies associations. Unchannelized sheet-forms

are numerous while few channel-forms occur in the conglomeratic and sandy facies. On the other hand, the scarcity of Gcn, Gpt, Spt and Fm facies argues against the presence of standing water bodies in the alluvial fan and fluvial environments. These features suggest a sedimentation controlled by sudden and ephemeral flows. Another characteristic of the AG is the scarcity of silt and clay in the sediment matrix which can be linked to the dominance of volcanic and plutonic lithologies in the source-areas which limit the production of fine particles (Blair, 1999; Levson and Rutter, 2000) although it can also be related to a low efficiency of the weathering processes. This last hypothesis is in agreement with the presence of faceted pebbles, pedogenetic carbonate and the very rare indications of colonization by vegetation which suggest a relatively arid climate. Finally, the proximal origin of clasts (from the Precordillera and Central Depression) and the maximal preservation of sediments in the Precordillera (about 500 m) decreasing westward (less than 200 m) are evidences for a limited capacity of sediment transport in river beds.

All these features are, as suggested by numerous authors (Hartley and May, 1998; Hartley, 2003; Hinojosa, 2005; Rech et al., 2006), in agreement with the prevalence of semi-arid to arid climatic conditions along this section of the Atacama Desert since at least the Lower Miocene. These conditions favour chemical precipitation and particularly the formation of gypcretes (Watson, 1989; Hartley and May, 1998). Evaporite minerals are relatively uncommon in the AG where they are represented by some gypsum-filled cracks (e.g. A2 association) or halite and gypsum crystals within clay layers (A5 association). This scarcity suggests a lack of standing water bodies and limited water circulation in the vadose and upper phreatic zones. The lateral transition of facies associations (proximal - distal), the palaeocurrent directions and the bedding dips are consistent with overall drainage to the west, extending across and beyond the Atacama Fault, in the Coastal Cordillera A connection with the ocean could explain the low abundance of evaporitic facies, even though the climatic conditions were favourable for their formation.

Contemporaneously with the deposition of the AG, deformation linked to tectonic shortening occurred at Cordillera Claudio Gay (Mpodozis and Clavero, 2002), and further to the east in the Argentine Puna (Kraemer et al., 1999; Voss, 2003). The sediment flux resulting from the exhumation of these domains was mainly trapped in the endoreic Pre Andean Depression (Riquelme et al., 2003) and had little effect on sedimentation in the Central Depression. No evidence of significant Neogene to Quaternary deformation has been found in the Precordillera or the Central Depression (i. e. Cornejo et al, 1993, 1999; Godoy and Lara, 1998; Audin et al, 2003) where, along the studied transect undeformed

AG deposits overlie the Eocene to early Oligocene thrusts of the Potrerillos Fold and Thrust Belt and the Sierra del Castillo and Agua Amarga faults.

Riquelme et al. (2003, 2007), indicated that accumulation and preservation of the Atacama Gravels was, related to the Neogene activity on the AFS, producing uplift of the western part of the Coastal Cordillera which acted as a barrier to rivers flowing to the west from the Precordillera. Our observations of the AFS near El Salado (log 12, Figs. 2, 6) show, however, that, although “young” normal faults actually cut and displace the Atacama Gravels and an overlying alluvial fan, the lack of thickness and/or facies changes eastward of the AFS disagrees with the hypothesis of active faulting during or immediately before deposition of the Miocene gravels. Along the whole studied transect we have been unable to find any evidence of Miocene synsedimentary deformation (e.g. progressive unconformities or thickness variations). Dip in beds of the A1-A2 facies association in the Precordillera is around 2-3°, which is compatible with the depositional profile of an arid alluvial fan (Nilsen, 1982; Blair and McPherson, 1994), not modified by post sedimentary deformation. A rough estimation of sedimentation rates controlled by the available radiometric dates in log 1 (about 8 m/Ma) is also incompatible with active tectonic subsidence during AG sedimentation.

Minor Neogene deformation was therefore unable to create enough subsidence to permit the deposition and preservation of the Atacama Gravels. On the other hand, the sedimentological analysis indicates limited water flow during sediment deposition, in better agreement with the hypothesis that AG preservation was the result of low sediment-carrying capacity of the rivers as a consequence of the changing climatic conditions in the Atacama Desert all through the Miocene.

5.2. Model for the evolution of the Atacama Gravels

During the Eocene to early Oligocene, the exhumation and uplift of the Precordillera caused the incision of deep paleovalleys (Fig. 6 and 8a) (Maksaev and Zentilli, 1999; Nalpas et al., 2005). Although climatic conditions remained arid or semi-arid since at least the late Eocene, there were intermittent periods of relatively high rainfall (e.g. 34 Ma, 25 Ma and 20 Ma; Alpers and Brimhall, 1988, 1989; Dunai et al., 2005; Hinojosa, 2005; Arancibia et al., 2006). The smooth paleovalley surfaces, fossilized below the gravels, are formed during these relatively wet climatic episodes. The resulting high river discharge was the cause of the active transfer of sediments from the Precordillera to the Pacific across the Coastal Cordillera.

During the Miocene a progressive increase of aridity (Hinojosa, 2005) induced a fall of fluvial transport capacity limiting the mass transfer to the ocean and initiating the sedimentation / preservation of the proximal facies association (A1-A2) of the AG along the paleovalley system (Fig. 8b). Considering the preservation of gravels (A1-A2 associations) below the Los Cristales ignimbrite (16.6 Ma), and calculated sedimentation rates (log 1, A3 association, around 8 m/Ma), we propose that AG sedimentation began during the late Oligocene-early Miocene. A temporal trend towards increasing aridity is shown by the increased roughness of the basement surface below the gravel contact along the upper part of the paleovalley slopes, due as a consequence of decreasing water flow. The sediments here lie on top of the pediment, exhibiting more distal facies (A3-A4-A5, Fig. 8C). The topography is smoothed in relation with a desert burial by debris coming from the weathering of the bedrock during middle Miocene.

As climatic conditions became hyper-arid around 9-10 Ma (Hartley and May, 1998), both sedimentation and erosion came to a halt. The preservation of the pediment surface exposed since 9 Ma (Nishiizumi et al., 2005), which seals the Atacama Gravels in the Precordillera, is in good agreement with the evolution of climate towards hyper aridity during the Late Miocene. Sedimentation/preservation of thin alluvial fan deposits continued after 9 Ma in the Central depression and Coastal Cordillera, but seems to have totally ceased at around 6 Ma (Fig. 6, log 12).

6. Conclusions

- New ^{39}Ar - ^{40}Ar ages data obtained from the ignimbrite layers intercalated in the Atacama along the Chañaral-Potrerrillos transect (Los Cristales: 16.3 Ma, Ignimbrite, San Andrés: 9.1-9.2 Ma) confirm K/Ar ages previously published. A third, up to now unrecognized ignimbrite, found on top of alluvial fan deposits on the Coastal Cordillera was dated at 5.9-6.0 Ma. These radiometric data, and the evolution of late Oligocene and Miocene climatic conditions, permit to place the beginning of AG sedimentation at the Oligocene-Miocene boundary, and its cessation during the late Miocene
- Five facies associations, which form the bulk of the Atacama Gravels along the Chañaral-Pedernales transect, indicate sedimentary processes on alluvial fan, ephemeral fluvial and playa lake environments. Lateral correlations indicate a general E-W facies change trend, from predominantly proximal alluvial fan facies associations in the Precordillera and the eastern part of the Central Depression to distal, ephemeral fluvial and playa-lake facies

associations along the eastern border of the Coastal Cordillera, and in the Rio Salado paleovalley along the Coastal Cordillera.

- An important change on the mass transfer regime occurred between the Oligocene, when all the sediments are exported out of the drainage system towards the ocean, and the Miocene, when the sediments started to accumulate along the drainage network. AG deposits preserved along of the Rio Salado catchment represent the infill of a drainage system converging to a canyon outlet open towards the Pacific Ocean, indicating exoreic conditions during sedimentation.

- The lack of evidences of synsedimentary deformation, together with the sedimentological evidence of deposition under semi-arid to arid conditions, enable us to link the sedimentation and preservation of the Atacama Gravels with a progressive climatic shift towards aridity. Increasing aridity during the Miocene lowered the sediment transport capacity of fluvial channels, and triggering the infilling of paleovalleys. The sediment accumulation stopped during the Late Miocene when hyper-arid climatic conditions were finally reached.

Acknowledgements

The authors thank the French IRD (Institut de Recherche pour le Developpement) and ECOS-Chile program n° CO5U04 for financial support, C. Arriagada, L. Pinto, R. Riquelme and P. Roperch are gratefully acknowledged for constructive discussions. M.S.N. Carpenter post-edited the English style.

References

- Allmendinger, R. W., Jordan, T. E., Kay, S. M., Isacks, B., 1997. The Evolution of the Altiplano-Puna Plateau of the Central Andes. *Annual Review of Earth and Planetary Sciences* 25, 139-174.
- Alpers, C.N., Brimhall, G.H., 1988. Middle Miocene climatic change in the Atacama Desert, northern Chile: Evidence from supergene mineralisation at La Escondida. *Geological Society of America Bulletin* 100, 1640-1656.
- Alpers, C.N., Brimhall, G.H., 1989. Paleohydrologic evolution and geochemical dynamics of cumulative supergene metal enrichment at La Escondida, Atacama Desert, northern Chile. *Economic Geology* 84, 229-255.
- Arancibia, G., Matthews, S.J., Pérez de Arce, C., 2006. K–Ar and $^{40}\text{Ar}/^{39}\text{Ar}$ geochronology of supergene processes in the Atacama Desert, Northern Chile: tectonic and climatic relations. *Journal of the Geological Society of London* 163, 107-118.
- Arriagada, C., Roperch, P., Mpodozis, C., Fernández, R., 2006. Paleomagnetism and tectonics of the southern Atacama Desert region (25-28°S), Northern Chile. *Tectonics* 25, TC1008.
- Audin, L., Hérial, G., Riquelme, R., Darrozes, J., Martinod, J., Font, E., 2003. Geomorphological markers of faulting and neotectonic activity along the western Andean margin, Northern Chile. *Journal of Quaternary Science* 18, 681-694.
- Avouac, J.P., Burov, E.B., 1996. Erosion as a driving mechanism of intracontinental mountain growth. *Journal of Geophysical Research* 101, 17747-17769.
- Baby, P., Rochat, P., Mascle, G., Hérial, G., 1997. Neogene shortening contribution to crustal thickening in the back arc of the Central Andes. *Geology* 25, 883-886.
- Baumont, C., Fullsack, P., Hamilton, J., 1992. Erosional control of active compressional orogens. In: McClay, K.R. (Ed.), *Thrust tectonics*. Chapman & Hall, London, pp. 1-18.
- Blair, T.C., 1999. Cause of dominance by sheetflood vs. debris-flow processes on two adjoining alluvial fans, Death Valley, California. *Sedimentology* 46, 1015-1028.
- Blair, T.C., McPherson, J.G., 1994. Alluvial fans and their natural distinction from rivers based on morphology, hydraulic processes, sedimentary processes and facies assemblages. *Journal of Sedimentary Research* A64, 450-489.
- Bordy, E.M., Catuneanu, O., 2001. Sedimentology of the upper Karoo fluvial strata in the Tuli Basin. *Journal of African Earth Sciences* 33, 605-629.

- Brown, M., Díaz, F., Grocott, J., 1993. Displacement history and tectonic significance of the El Salado segment of the Atacama Fault System, Northern Chile. *Geological Society of America Bulletin* 105, 1165-1174.
- Chough, S.K., Hwang, I.G., Choe, M.Y., 1990. The Miocene Doumsan fan-delta, southeast Korea: a composite fan-delta system in a back-arc margin. *J. sedim. Petrol.*, 60, 445-455.
- Clark, A.H., Mortimer, C., Sillitoe, R., 1967. Implications of the isotopic ages of ignimbrite flows, southern Atacama Desert, Chile. *Nature* 215, 723-724.
- Clavero, J., Mpodozis, C., Gardeweg, M., 2000. La caldera Wheelwright, una estructura volcánica circular en la zona sur de la cadera volcánica los Andes centrales (región de Atacama, Chile). IX Congreso Geológico Chileno, Actas 2, pp. 274.
- Coira, B., Davidson, J., Mpodozis, C., Ramos, V.A., 1982. Tectonic and magmatic evolution of the Andes of northern Argentina and Chile. *Earth Science Reviews* 18, 303-332.
- Collinson, J.D., 1986. Alluvial sediments. In: Reading, H.G. (Ed.), *Sedimentary environments and facies*. Blackwell, Oxford, pp. 37-82.
- Cornejo, P., Mpodozis, C., Matthews, S. 1999. Geología y Evolución Magmática del Distrito Indio Muerto y Yacimiento El Salvador. Servicio Nacional de Geología y Minería, Informe Registrado IR-98-14, 99 p.
- Cornejo, P., Mpodozis, C., Ramírez, C. F., Tomlinson, A.J., 1993. Estudio Geológico de la región de El Salvador y Potrerillos. Servicio Nacional de Geología y Minería, Santiago de Chile, Informe Registrado IR 93-1, 358 p.
- Cornejo, P., Riquelme, R., Mpodozis, C., 1998a. Mapa Geológico de la Hoja Salvador, Región de Atacama. Escala 1:100.000, versión preliminar: Servicio Nacional de Geología y Minería, Santiago de Chile.
- Cornejo, P., Tosdal, R., Mpodozis, C., Tomlinson, A.J., 1998b. Hoja Salar de Maricunga, Región de Atacama. Mapas Geológicos 7, Escala 1:100.000. Servicio Nacional de Geología y Minería, Santiago de Chile.
- Cornejo, P., Tosdal, R.M., Mpodozis, C., Tomlinson, A.J., Rivera, O., Fanning, C.M., 1997. El Salvador Porphyry Copper revisited: Geologic and geochronologic Framework. *International Geology Review* 39, 22-54.
- Coutand, I., Cobbold, P., Urreiztieta, M., Gautier, P., Chauvin, A., Gapais, D., Rosello, E.A., Lopez-Gamundi, O., 2001. Style and history of Andean deformation, Puna plateau, northwestern Argentina. *Tectonics* 20, 210-234.

- Dallmeyer, R., Brown, M., Grocott, V., Taylor, G., Treloar, P., 1996, Mesozoic magmatic and tectonic events within the Andean Plate Boundary Zone, 26°-27°30'S, North Chile: constrain from $^{40}\text{Ar}/^{39}\text{Ar}$ mineral ages. *Journal of Geology*, 104, 19-40.
- Dunai, T.J., González López, G.A., Juez-larré, J., 2005. Oligocene-Miocene age of aridity in the Atacama Desert revealed by exposure dating of erosion-sensitive landforms. *Geology* 33, 321-324.
- Echavarría, L., Hernández, R., Allmendinger, R., Reynolds, J., 2003. Subandean thrust and fold belt of northwestern Argentina: Geometry and timing of the Andean evolution AAPG Bulletin, v. 87, no. 6, 965-985.
- Gabalda, G., Nalpas, T., Bonvalot, S., 2005. Base of the Atacama Gravels Formation (26°S, Northern Chile): first results from gravity data. Sixth International Symposium on Andean Geodynamics, Barcelona, Spain. IRD Editions, extended abstracts, pp. 286-289.
- Garzione, C.N., Molnar, P., Libarkin, J.C., MacFadden, B.J., 2006. Rapid late Miocene rise of the Bolivian Altiplano: Evidence for removal of mantle lithosphere. *Earth and Planetary Science Letters* 241, 543-556.
- Ghibaudo, G., 1992. Subaqueous sediment gravity flow deposits: practical criteria for their field description and classification. *Sedimentology* 39, 423-454.
- Godoy, E., Lara, L., 1998. Hojas Chañaral y Diego de Almagro, Región de Atacama. Mapas Geológicos 5-6, Escala 1:100.000. Servicio Nacional de Geología y Minería, Santiago de Chile.
- Ghosh, P., Garzione, C.N., Eiler, J.M., 2006. Rapid Uplift of the Altiplano Revealed Through ^{13}C - ^{18}O Bonds in Paleosol Carbonates. *Science* 311, 511-515.
- Gregory-Wodzicki, K.M., 2000. Uplift history of the Central and Northern Andes: A review. *Geological Society of America Bulletin* 112, 1091-1105.
- Grocott, J., Taylor, G.K., 2002. Magmatic arc fault systems, deformation partitioning and emplacement of granitic complexes in the Coastal Cordillera, north Chilean andes (25°30'S to 27°00'S). *Journal of the Geological Society of London* 159, 425-442.
- Gubbels, T., Isacks, B., Farrar, E., 1993. High-level surfaces, plateau uplift, and foreland development, Bolivian central Andes. *Geology* 21, 695-698.
- Hanes, J.A., York, D., Hall, C.M., 1985. An $^{40}\text{Ar}/^{39}\text{Ar}$ geochronological and electron microprobe investigation of an Archean pyroxenite and its bearing on ancient atmospheric compositions. *Can. J. Earth. Sci.*, 22: 947-958.
- Hartley, A.J., 2003. Andean uplift and climate change. *Journal of Geological Society*, London, vol. 160, 7-10.

- Hartley, A.J., May, G., 1998. Miocene Gypcretes from the Calama Basin, northern Chile. *Sedimentology* 45, 351-364.
- Hartley, A.J., May, G., Chong, G., Turner, P., Kape, S.J. Jolley, E.J., 2000. Development of a continental fore-arc: A Cenozoic example from the Central Andes, northern Chile. *Geology* 28, 331-334.
- Hinojosa, L., 2005. Cambios climáticos y vegetacionales inferidos a partir de paleofloras cenozoicas del sur de Sudamérica. *Revista Geológica de Chile* 32, 95-115.
- Horton, B.K., Schmitt, J.G., 1996. Sedimentology of the lacustrine fan-delta system, Miocene Horse Camp Formation, Nevada, USA. *Sedimentology* 43, 133-155.
- Iriarte, S., Arévalo, C., Mpodozis, C., Rivera, O., 1996. Hoja Carrera Pinto, Región de Atacama. Mapas Geológicos 3, Escala 1:100.000. Servicio Nacional de Geología y Minería, Santiago de Chile.
- Kay, S.M., Mpodozis, C., Coira, B., 1999. Neogene magmatism, tectonism and mineral deposits of the Central Andes (22°-33°S latitude). In: Skinner, B.J. (Ed.), *Geology and Ore Deposits of the Central Andes*. Society of Economic Geologists, Special Publication 7, pp. 27-59.
- Kley, J., Monaldi, C.R., Salfity, J.A., 1999. Along-strike segmentation of the Andean foreland: causes and consequences. *Tectonophysics* 301, 75-94.
- Kocurek, G., Hunter, R.E., 1986. Origin of polygonal fractures in sand, uppermost Navajo and Page Sandstones, Page, Arizona. *Journal of Sedimentary Research* 56, 895-904.
- Kraemer, B., Aldeman, D., Alten, M., Schnurr, W., Erpenstein, K., Kiefer, E., van den Bogaard, P., Görler, K., 1999. Incorporation of the Paleogene foreland into the Neogene Puna plateau: The Salar de Antofalla area, NW Argentina. *Journal of South American Earth Sciences* 12, 157-182.
- Lamb, S., Davis, P., 2003. Cenozoic climate change as a possible cause for the rise of the Andes. *Nature* 425, 792-797.
- Lara, L., Godoy, E., 1998. Hoja Quebrada Salitrosa, Región de Atacama. Mapas Geológicos 4, Escala 1:100.000. Servicio Nacional de Geología y Minería, Santiago de Chile.
- Leturmy, P., Mugnier, J.L., Vinour, P., Baby, P., Coletta, B., Chabron, E., 2000. Piggyback basin development above a thin-skinned thrust belt with two detachments levels as a function of interactions between tectonic and superficial mass transfer: The case of the Subandean Zone (Bolivia). *Tectonophysics* 320, 45-67.

- Levson, V.M., Rutter, N.W., 2000. Influence of bedrock geology on sedimentation in Pre-Late Wisconsinan alluvial fans in the Canadian Rocky Mountains. *Quaternary International* 68-71, 133-146.
- Maksaev, V., Zentilli, M., 1999. Fission track Thermochronology of the Domeyko Cordillera, Northern Chile: Implications for Andean Tectonics and Porphyry Copper Metallogenesis. *Exploration and Mining Geology Journal* 8, 65-89.
- McQuarrie, N., Horton, B.K., Zandt, G., Beck, S., DeCelles, P.G., 2005. Lithospheric evolution of the Andean fold-thrust belt, Bolivia, and the origin of the central Andean Plateau. *Tectonophysics* 399, 15-37.
- Miall, A.D., 1977. A review of the braided river depositional environment. *Earth-Science Reviews* 13, 1-62.
- Miall, A.D., 1996. *The Geology of Fluvial Deposits - Sedimentary Facies, Basin Analysis and Petroleum Geology*. Springer, Berlin, 582 p.
- Molnar, P., England, P., 1990. Late Cenozoic uplift of mountain ranges and global climate change: Chicken or egg? *Nature* 346, 29-34.
- Montgomery, D.R., Balco, G., Willett, S.D., 2001. Climate, tectonics, and the morphology of the Andes. *Geology* 29, 579-582.
- Mortimer, G., 1973. The Cenozoic history of the southern Atacama Desert, Chile. *Journal of the Geological Society of London* 129, 505– 526.
- Mpodozis, C., Ramos, V.A., 1989. The Andes of Chile and Argentina. In: Fricksen, G.E., Cañas Pinochet, M.T., Reinemund, J.A. (Eds.), *Geology of the Andes and its relation to hydrocarbon and mineral resources*. Circum-Pacific Council for Energy and Mineral Resources Earth Science Series 11, 59-89.
- Mpodozis, C., Clavero, J., 2002. Tertiary Tectonic evolution of the southwestern edge of the Puna Plateau: Cordillera Claudio Gay (26°-27°S). Fifth International Symposium on Andean Geodynamics, Toulouse, France. IRD Editions, extended abstracts, pp. 445-448.
- Mpodozis, C., Tomlinson, A., Cornejo, P., 1994. Acerca del control estructural de intrusivos eocenos y pórfidos en la región de Potrerillos, El Salvador. VII Congreso Geológico Chileno, Actas 2, pp. 1596-1600.
- Mpodozis, C., Cornejo, P., Kay, S.M., Tittler, A., 1995. La Franja de Maricunga: Síntesis de la evolución del frente volcánico oligoceno-mioceno de la zona sur de los Andes Centrales. *Revista Geológica de Chile* 22, 273–314.
- Mulder, T., Alexander, J., 2001. The physical character of subaqueous sedimentary density flows and their deposits. *Sedimentology* 48, 269-299.

- Mugnier, J.L., Baby, P., Coletta, B., Vinour, P., Balé, P., Leturmy, P., 1997. Thrust geometry controlled by erosion and sedimentation: A view from analogue models. *Geology* 25, 427-430.
- Nalpas, T., Hérail, G., Mpodozis, C., Riquelme, R., Clavero, J., Dabard, M.P., 2005. Thermochronological data and denudation history along a transect between Chañaral and Pedernales ($\approx 26^\circ$ S), north Chilean Andes: orogenic implications. Sixth International Symposium on Andean Geodynamics, Barcelona, Spain. IRD Editions, extended abstracts, pp. 548-551.
- Nalpas, T., Gapais, D., Verges, J., Barrier, L., Gestain, G., Leroux, G., Rouby, D., Kermarrec, J.J., 2003. Effects of rate and nature of synkinematic sedimentation on the growth of compressive structures constrained by analogue models and field examples. *Geological Society of London Special Publication* 208, 307-319.
- Nemec, W., Postma, G., 1993. Quaternary alluvial fans in Crete. In: Marzo, M., Puigdefabregas, C. (Eds.), *Alluvial Sedimentation*. International Association of Sedimentologists Special Publication 17, 235-276.
- Nilsen, T.H., 1982. Alluvial fan deposits. In: Sholle, P.A., Spearing, D. (Eds.), *Sandstone Depositional Environments*. American Association of Petroleum Geologists Memoirs 31, 49-86.
- Nishiizumi, K., Caffee, M.W., Finkel, R.C., Brimhall, G., Mote, T., 2005. Remnants of a fossil alluvial fan landscape of Miocene age in the Atacama Desert of northern Chile using cosmogenic nuclide exposure age dating. *Earth and Planetary Science Letters* 237, 499-507.
- Pardo-Casas, F., Molnar, P., 1987. Relative motion of the Nazca (Farallon) and South American plates since Late Cretaceous time. *Tectonics* 6, 233-248.
- Rech, J.A., Currie, B.S., Michalski, G., Cowan, A.M., 2006. Neogene climate change and uplift in the Atacama Desert, Chile, *Geology*, 34, 761-764.
- Renne, P. R., Swisher, C. C., Deino, A. L., Karner, D. B., Owens, T. L., DePaolo, D. J. 1998. Intercalibration of standards, absolute ages and uncertainties in $^{40}\text{Ar}/^{39}\text{Ar}$ dating. *Chemical Geology*, 145, 117-152.
- Riquelme, R., 2003. Evolution géomorphologique néogène des Andes centrales du Désert d'Atacama (Chili) : interactions tectonique-érosion-climat. Toulouse (France) et Santiago (Chili), Thèse de troisième cycle, 258 p.
- Riquelme, R., Martinod, J., Hérail, G., Darrozes, J., Charrier, R., 2003. A geomorphological approach to determining the Neogene to Recent tectonic

deformation in the Coastal Cordillera of northern Chili (Atacama). *Tectonophysics* 361, 255-275.

- Riquelme, R., Hérail, G., R., Martinod, J., Charrier, R., Darrozes, J., 2007. Late Cenozoic geomorphologic signal of Andean forearc deformation and tilting associated with the uplift and climate changes of the Southern Atacama Desert (26°S–28°S). *Geomorphology* 86, 283-306.
- Roddick, J. C., Cliff, R. A., Rex D. C., 1980. The evolution of excess argon in alpine biotites- ^{40}Ar - ^{39}Ar analysis. *Earth Planet. Sci. Lett.*, 48: 185-208.
- Ruffet, G., Féraud, G., Balèvre, M., Kiénast, J.-R., 1995. Plateau ages and excess argon in phengites: an ^{40}Ar - ^{39}Ar laser probe study of Alpine micas (Sesia Zone, Western Alps, northern Italy). *Chemical Geology (Isotopic Geoscience Section)* 121, 327-343.
- Ruffet, G., Gruau, G., Ballèvre, M., Féraud, G., Philippot, P., 1997. Rb-Sr and ^{40}Ar - ^{39}Ar laser probe dating of high-pressure phengites from the Sesia zone (western Alps): underscoring of excess argon and new age constraints on the high-pressure metamorphism. *Chemical Geology* 141, 1-18.
- Sillitoe, R.H., Mortimer, C., Clark, A.H., 1968. A chronology of landform evolution and supergene mineral alteration, Southern Atacama Desert, Chile. *Institution of Mining and Metallurgy, Transactions B77*, 166-169.
- Smith, G.A., 1986. Coarse-grained nonmarine volcanoclastic sediment: Terminology and depositional process. *Geological Society of America Bulletin* 97, 1-10.
- Spalletti, L.A., Piñol, F.C., 2005. From Alluvial Fan to Playa: An Upper Ephemeral Fluvial System, Neuquén Basin, Argentina. *Gondwana Research* 8, 363-383.
- Summerfield, M.A., Hulton, N.J., 1994. Natural controls of fluvial denudation rates in major world drainage basins. *Journal of Geophysical Research* 99, 13871-13883.
- Svendsen, J., Stollhofen, H., Krapf, C.B.E., Stanistreet, I.G., 2003. Mass and hyper-concentrated flow deposits record dune damming and catastrophic breakthrough of ephemeral rivers, Skeleton Coast Erg, Namibia. *Sedimentary Geology* 160, 7-31.
- Tomlinson, A.J., Cornejo, P., Mpodozis, C., 1999. Hoja Potrerillos, Región de Atacama. *Mapas Geológicos* 14, Escala 1:100.000. Servicio Nacional de Geología y Minería, Santiago de Chile.
- Tomlinson, A.J., Mpodozis, C., Cornejo, P., Ramírez, C.F., Dumitri, T., 1994. El sistema de Fallas Sierra de Castillo-Agua Amarga: Transpresión sinistral eocena en la precordillera de Potrerillos, El Salvador. *VII Congreso Geológico Chileno, Actas* 2, pp. 1459-1463.
- Turner, G., 1971. ^{40}Ar - ^{39}Ar ages from the lunar Maria. *Earth Planet. Sci. Lett.*, 11: 169-191.

- Uba, C.E., Heubeck, C., Hulka, C., 2005. Facies analysis and basin architecture of the Neogene Subandean synorogenic wedge, southern Bolivia. *Sedimentary Geology* 180, 91-123.
- Voss, R., 2003. Cenozoic stratigraphy of the southern Salar de Antofalla region, northwestern Argentina. *Revista Geológica de Chile* 29, 167-189.
- Watson, A., 1989. Desert crusts and rock varnish. In: D.S.G. Thomas (Ed.) *Arid Zone Geomorphology*. Belhaven Press, London, pp. 25-55.
- Waresback, D.B., Turbeville, B.N., 1990. Evolution of a Plio-Pleistocene volcanogenic-alluvial fan: The Puye Formation, Jemez Mountains, New Mexico. *Geological Society of America Bulletin* 102, 298-314.
- York, D., 1969. Least squares fitting of a straight line with correlated errors. *Earth Planet. Sci. Lett.*, 5: 320-324.

Figures captions:

Figure 1: (a) Morphotectonic units making up of the westernmost part of the Andean Cordillera in northern Chile. (b) Digital Elevation Map with major drainage features, also showing the study area (box). (c) Regional cross-section as shown in (a).

Figure 2: Study area along the Rio Salado valley (white dashed line), showing locations of the sedimentary logs. The regional extent of the Atacama Gravels is marked in transparent grey (modified after geological maps in Cornejo et al., 1998a; Godoy and Lara, 1998; Tomlinson et al., 1999), over a Landsat image (courtesy of NASA, <https://zulu.ssc.nasa.gov/mrsid/>). The location of the dated ignimbrites is represented by a star (white for Los Cristalles, grey for San Andrés and black for the youngest). Palaeocurrent data are derived from imbricated clasts in gravel facies.

Figure 3: Outcrop photographs of the five facies associations. The names of the lithofacies are adapted from Miall (1996) and Horton and Schmitt (1996), and described in Table 1.

Figure 4: 3D diagrams representing the organisation of the five facies associations (A1 to A5), with their location on (a) a close-up of proximal depositional environments and (b) an overview of the Atacama Gravels, from proximal depositional environments to playa deposits.

Figure 5: a) Frequency diagram of all apparent ages and calculated plateau ages with errors at the 1σ level. b) to f) ^{39}Ar - ^{40}Ar age spectra. The age error bars for each temperature steps are at the 1σ level and do not include errors in the J-values. The errors in the J-values are included in the plateau age calculations.

Figure 6: Correlation between six sedimentary sections along a proximal to distal (right to left) profile (see Fig. 2 for location). The five facies associations distinguished by a color code are described in section 3.2. The 'local fans' in the western part of the profile are a coarse blanket covering the AG at a short distance from the outcrops of the Coastal Cordillera bedrock. The top of the six sections is aligned in the figure with the elevation of their upper surface of the AG (without vertical exaggeration) which decreases continuously toward the west.

Figure 7: Location of sections 1 and 3 in relation to the relief, the paleovalley and the paleoflow direction during the deposition of the AG (Landsat image, courtesy of NASA, <https://zulu.ssc.nasa.gov/mrsid/>).

Figure 8: Three stages in the history of the Central Depression. (a) Oligocene: incision of the relief during relatively wet climate conditions; formation of the paleo-valleys observed today. (b) Early Miocene: onset of deposition of the Atacama Gravels under arid conditions by debris-flow and sheetflood processes. (c) Middle Miocene: end of AG sedimentation under hyper-arid conditions.

Table 1: Mineralogical compositions of some sands.

Table 2: Description of the lithofacies of the Atacama Gravels. Facies codes are modified from Horton and Schmitt (1996) and Miall (1996) except for the L facies.

Table 3: Plateau ages and $^{36}\text{Ar}/^{40}\text{Ar}$ versus $^{39}\text{Ar}/^{40}\text{Ar}$ correlation results (Isochrone results). Error bars and errors on the results are at the 1σ level. The $(^{36}\text{Ar}/^{40}\text{Ar})_i$ and isochrone ages are both calculated from the intercept of the best-fit line (York, 1969) with the respective axis of the correlation plot. $\text{MSWD}=\text{SUMS}/(n-2)$; SUMS: minimum weighted sum of residuals; n: number of points fitted. See ignimbrite location in figure 2 (LC: Los Cristalles; SA: San Andrés).

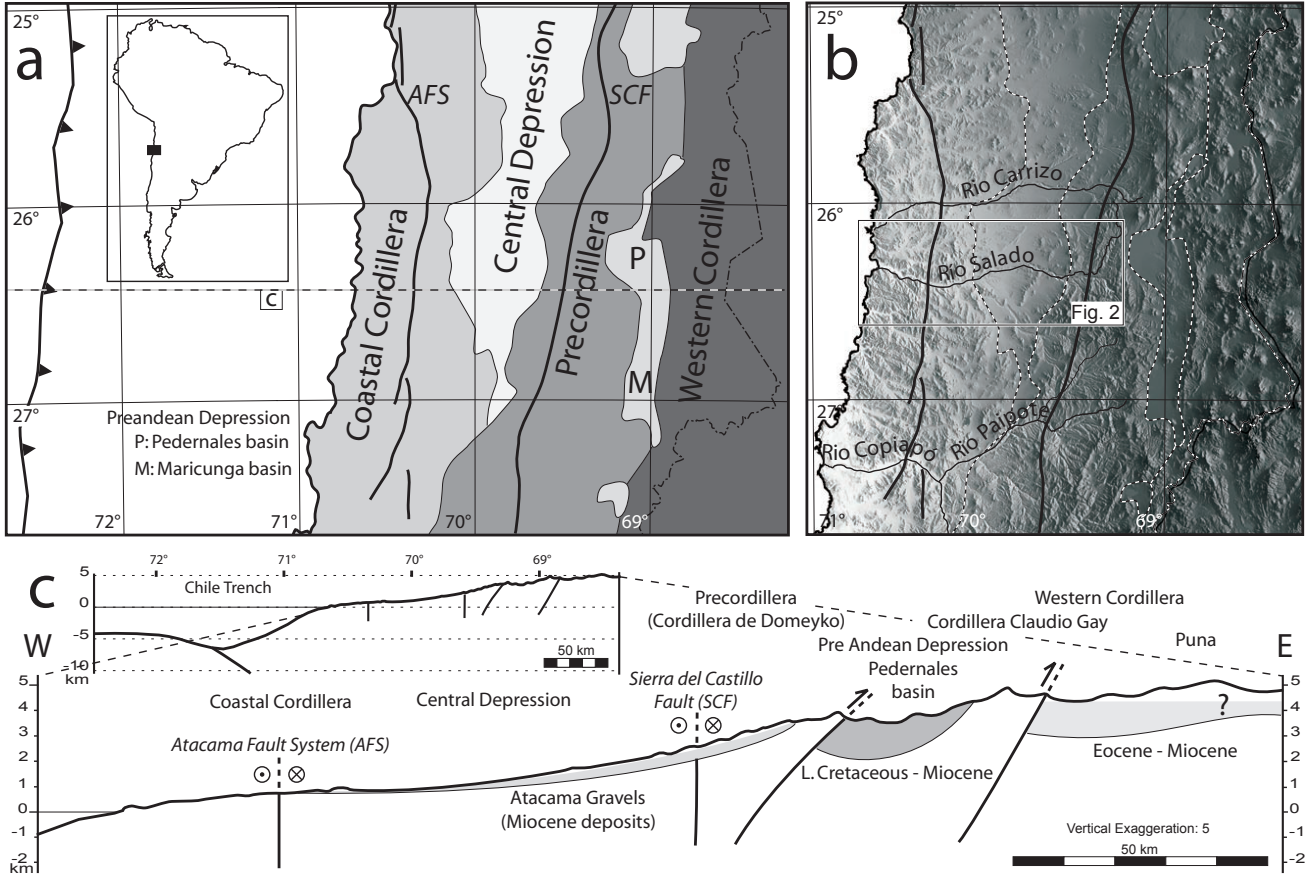


Fig. 1

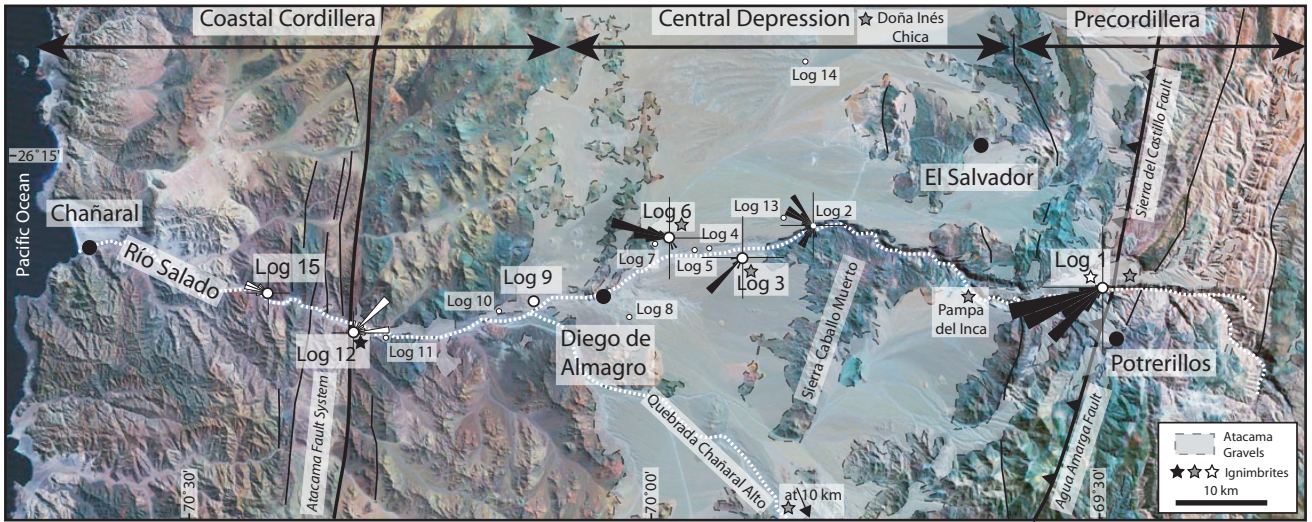
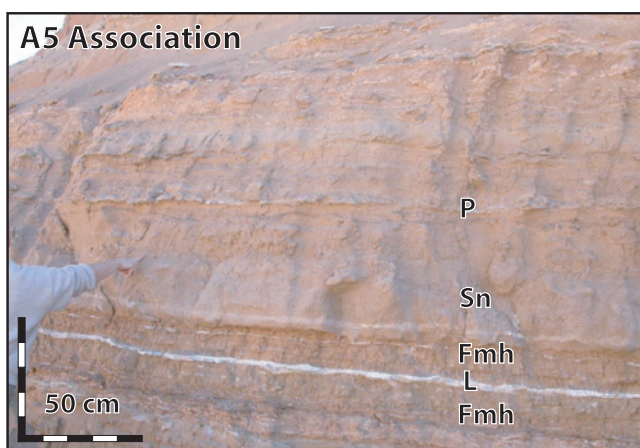
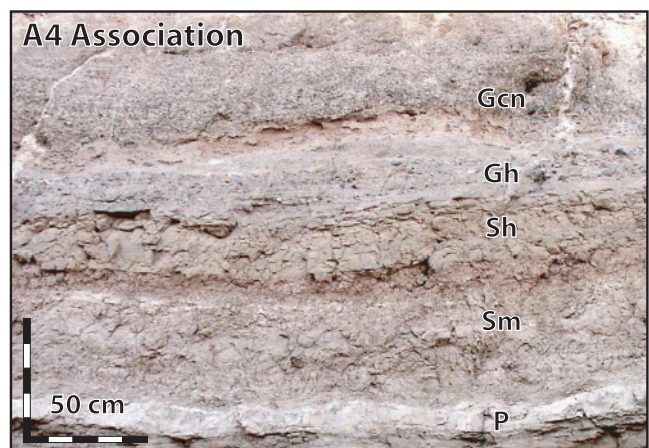
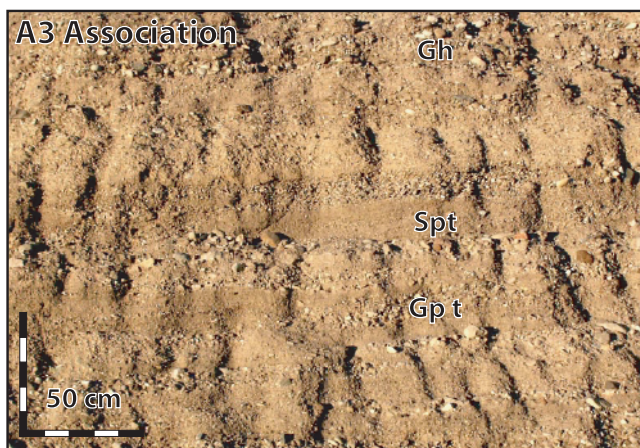
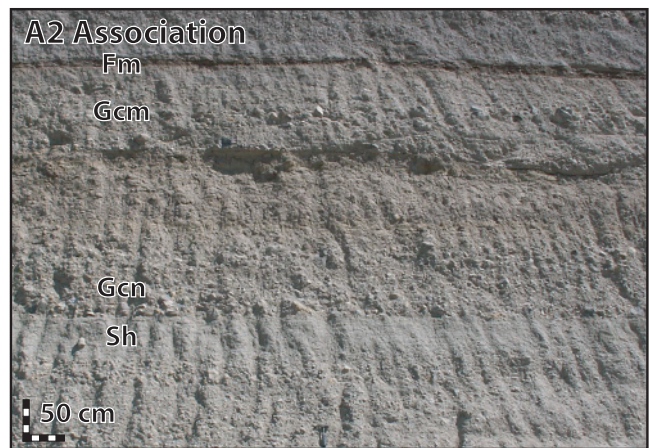
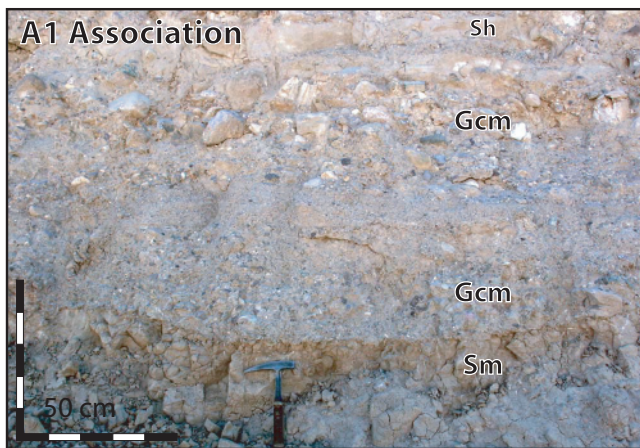


Fig. 2



Lithofacies:

- Gcm: clasts-supported, massive gravels
- Gcn: clasts-supported, normally graded gravels
- Gh: clasts-supported, horizontally stratified gravels
- Gp t: planar and trough cross-stratified gravels
- Spt: planar and trough cross-stratified sand
- Sn: normally graded sand
- Sh: horizontally laminated sand
- Sm: massive sand
- Fm: mud and silt
- Fmh: mud with halite
- L: detritic limestone
- P: pedogenetic carbonate

Fig. 3

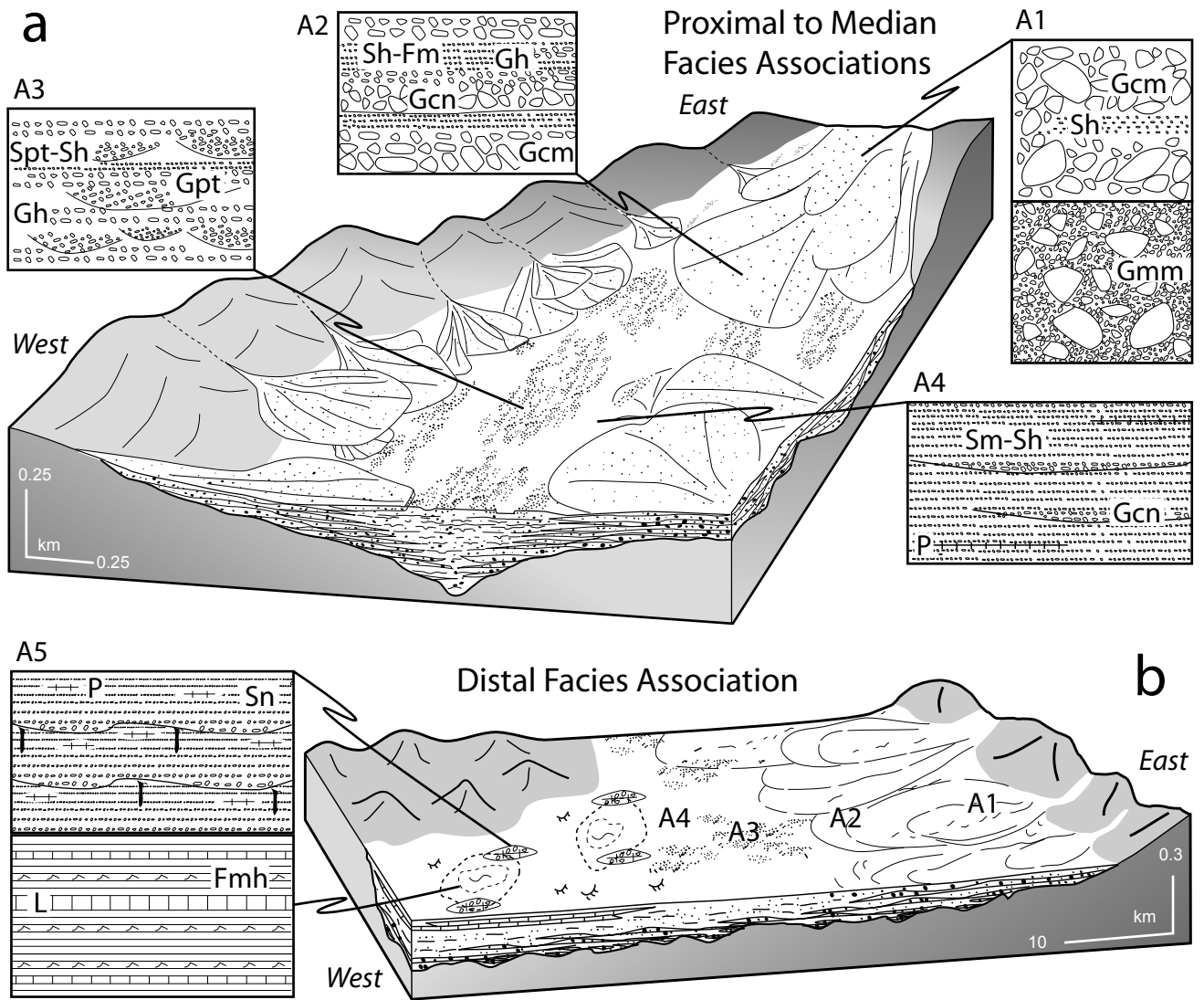


Fig. 4

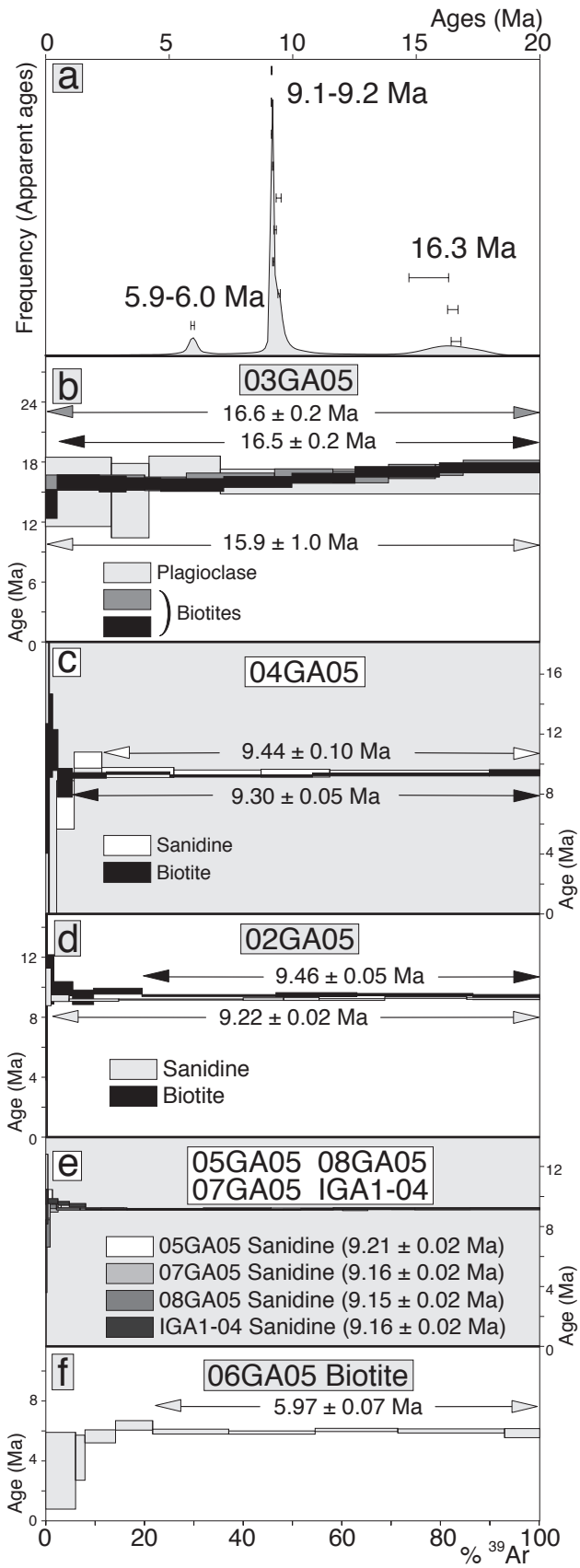


Fig. 5

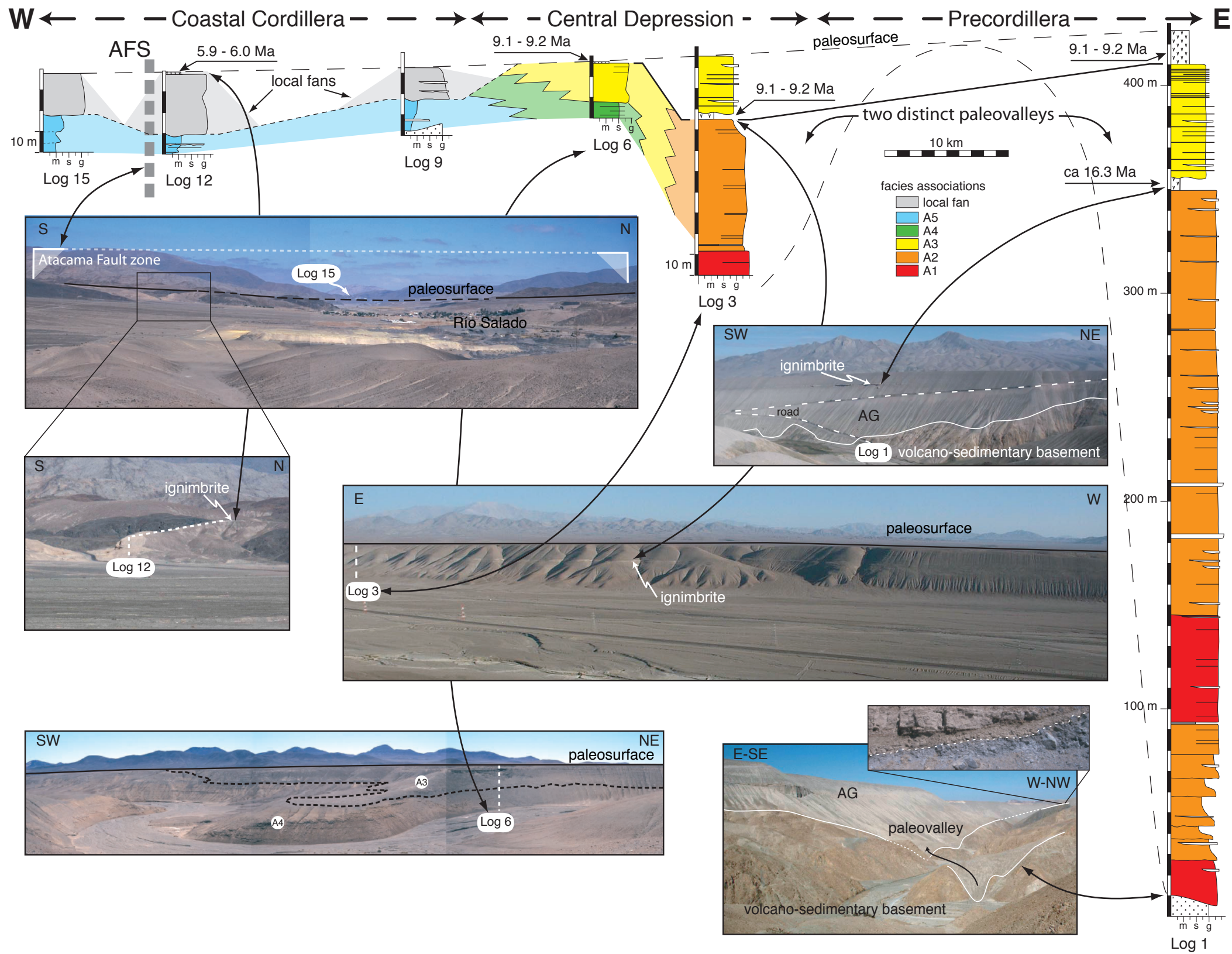


Fig. 6

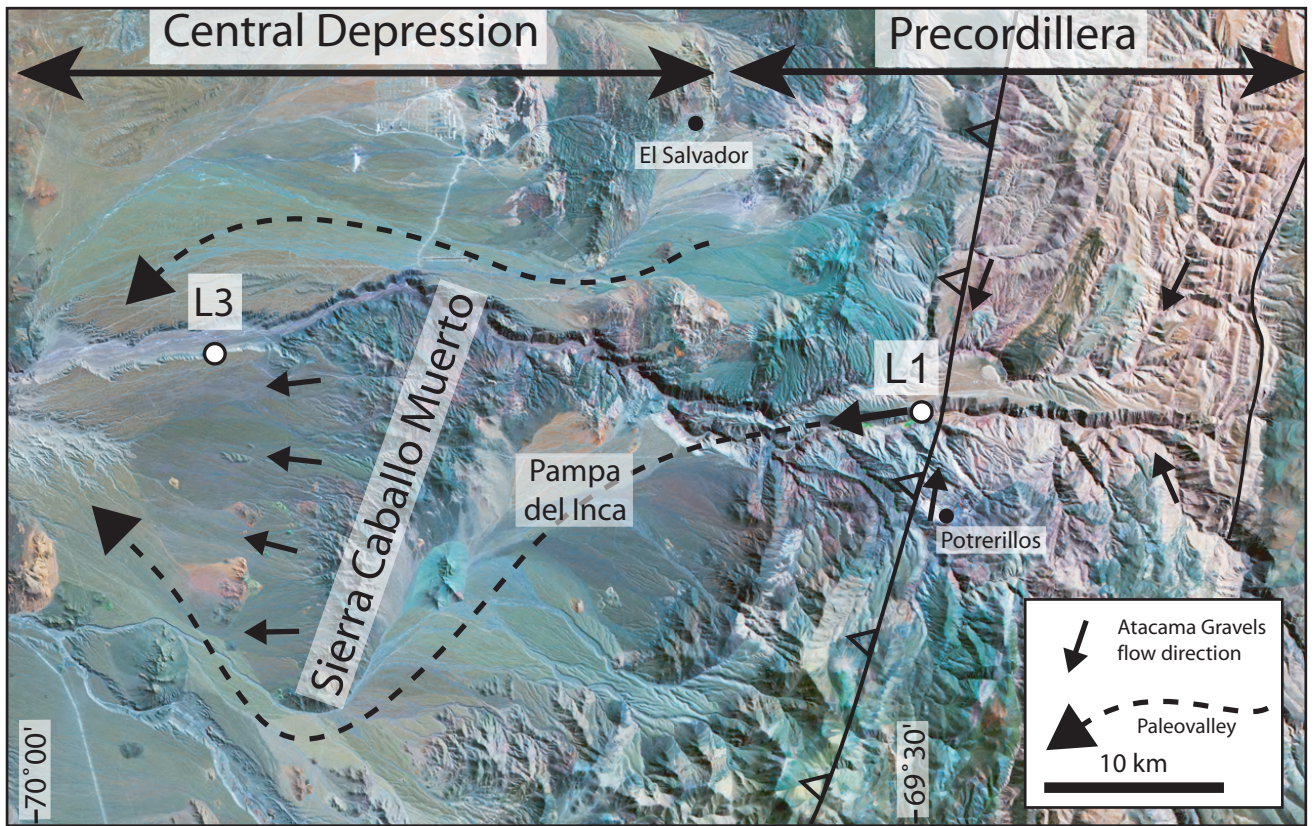


Fig. 7

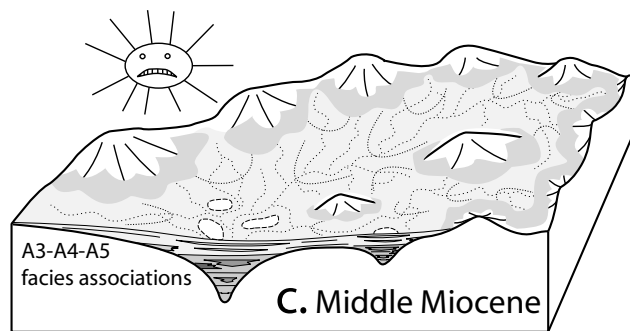
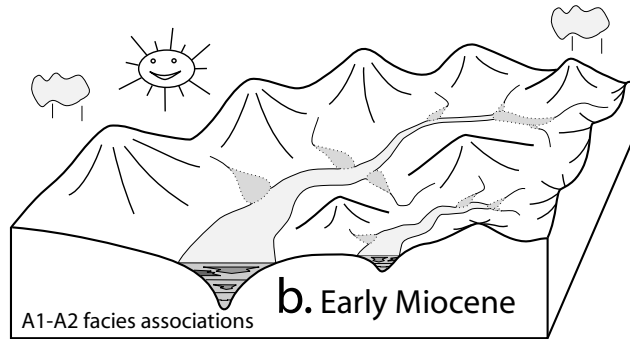
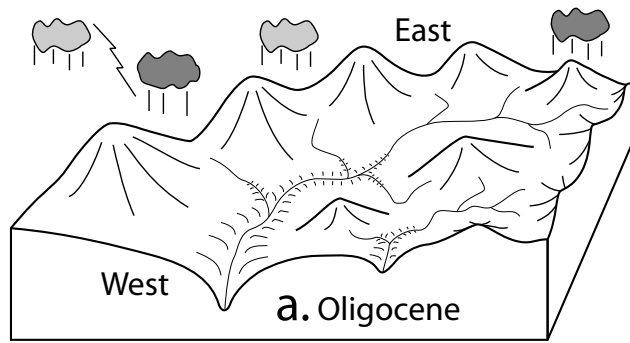


Fig. 8

Sample Location	Size	Composition
03AVG4 log 1	60 µm - 2 mm	- monocrystalline and polycrystalline quartz, plagioclase, biotite, epidote. - lithic fragments: volcanic rocks (felsitic rocks, hydrothermal) - calcareous cement
03AVG05 log 1	60 µm - 2 mm	- monocrystalline quartz, plagioclase - lithic fragments: limestone (micrite, oolitic limestones), magmatic and/or metamorphic rocks (quartz+feldspar) and volcanic rocks (felsitic grains, microlitic grains, lathwork grains, hydrothermal) - calcareous cement
03AVFA110 log 12	60 µm - 1 mm	- monocrystalline and polycrystalline quartz, plagioclase, K-feldspar, biotite, epidote. - lithic fragments: volcanic rocks (felsitic rocks, microlitic grains, lathwork grains, hydrothermal), magmatic and/or metamorphic rocks (quartz+K-feldspar, quartz + plagioclases, quartz + plagioclase + K-feldspar, quartz + micas), crystalline limestone - calcareous cement
03AVGA 290 log 12	60 µm - 700 µm	- monocrystalline and polycrystalline quartz, plagioclase, biotite, epidote. - lithic fragments: volcanic rocks (microlitic grains, hydrothermal), magmatic and/or metamorphic rocks (quartz + plagioclases) - calcareous cement
03AVFA 520 log 12		- monocrystalline quartz, biotite, plagioclase, K-feldspar, epidote - lithic fragments: volcanic rocks (felsitic rocks), magmatic and/or metamorphic rocks (quartz + feldspar) - calcareous cement

Facies	Description	Depositional processes
Gmm: matrix-supported, massive gravels	angular to sub-angular ungraded gravels (up to boulder size) in a silty to sandy matrix.	Plastic debris flows (Smith, 1986; Miall, 1996).
Gcm: clasts-supported, massive gravels	sub-angular to sub-rounded ungraded gravels (granules to cobbles) in a coarse sandy matrix.	Plastic or pseudo plastic debris flow (Miall, 1996); hyper concentrated flows (Smith, 1986; Horton and Schmitt, 1996).
Gcn: clasts-supported, normally graded gravels	sub-angular to sub-rounded gravels (granules to pebbles) showing a crude normal grading; few beds with horizontal alignment of clasts and few clast imbrications.	Hyperconcentrated flows (Waresback and Turbeville, 1990; Svendsen et al., 2003); high-density turbidity currents (Horton and Schmitt, 1996).
Gh: clasts-supported, horizontally stratified gravels	sub-rounded to rounded gravels (granules to pebbles) with horizontal to gently inclined stratification.	Upper-flow-regime condition (Waresback and Turbeville, 1990).
Gpt: planar and trough cross-stratified gravels	clast-supported gravels (mainly granules) with planar and trough cross stratification.	Upper part of lower-flow-regime conditions (Miall, 1996)
Spt: planar and trough cross-stratified sand	planar and trough cross-bedded sands with scattered pebbles (dm- to me-scale wavelength)	Lower-flow-regime conditions (Miall, 1996).
Sn: normally graded sand	normally graded coarse to fine sands with some bioturbation, granule particles common at the base of the bed.	Hyperconcentrated flows (Smith, 1986; Horton and Schmitt, 1996); High- or low-density turbidity currents (Ghibaudo, 1992).
Sh: horizontally laminated sand	fine to coarse well-sorted sand with scattered gravels; planar or sub-planar lamination	Lower part of the upper-flow-regime conditions (Collinson, 1996; Miall, 1996).
Sm: massive sand	ungraded and unstratified fine to coarse sand with scattered gravels	Hyper-concentrated flow (Smith, 1986; Mulder and Alexander, 2001); High density turbiditic currents (Chough et al., 1990)
Fm: mud, silt	massive or poorly laminated mud and silt with desiccation marks	Subaerial waning flood flows (Miall, 1977; Horton and Schmitt, 1996) and desiccation
Fmh: mud with halite	clay and salt with tepee structures	Suspension fallout and salt precipitation.
L: detritic limestone	carbonate micrite with ostracods bearing layers	Lacustrine conditions
P: pedogenetic carbonate	indurated carbonate horizons, (microsparite) locally with calcite-filled roots casts	Carbonate cementation from capillary groundwater flow (Miall, 1996).

Sample	Location	Mineral	Plateau age	Isochrone age	(⁴⁰Ar/³⁶Ar)_i	MSWD
03GA05	log 1 - LC	Biotite 1	16.6 ± 0.2	28.9 ± 0.9	246.4 ± 1.4 %	0.13
03GA05	log 1 - LC	Biotite 2	16.5 ± 0.2	21.3 ± 2.0	278.2 ± 2.7 %	2.02
03GA05	log 1 - LC	Plagioclase	15.5 ± 0.8	15.7 ± 1.1	299.6 ± 4.0 %	0.27
04GA05	log 1 - SA	biotite	9.30 ± 0.05	9.15 ± 0.11	295.3 ± 3.8 %	0.77
04GA05	log 1 - SA	sanidine	9.44 ± 0.10	9.25 ± 0.06	303.6 ± 0.6 %	0.09
08GA05	Pampa Inca	sanidine	9.15 ± 0.02	9.12 ± 0.02	299.2 ± 1.6 %	0.67
05GA05	Doña Inés Chica	sanidine	9.21 ± 0.02	9.19 ± 0.02	287.4 ± 11.6 %	0.54
07GA05	Chañaral Alto	sanidine	9.16 ± 0.02	9.14 ± 0.02	273.9 ± 14.3 %	0.64
02GA05	log 3	biotite	9.46 ± 0.05	9.34 ± 0.08	286.3 ± 10.1 %	1.43
02GA05	log 3	sanidine	9.22 ± 0.02	9.20 ± 0.03	299.3 ± 5.1 %	0.83
IGA1-04	log 6	sanidine	9.16 ± 0.02	9.13 ± 0.02	299.4 ± 1.7 %	0.56
06GA05	log 12	biotite	5.97 ± 0.07	5.86 ± 0.12	293.5 ± 3.3 %	0.69